

Enhancing Few-Shot Image Classification through Learnable Multi-Scale Embedding and Attention Mechanisms

Fatemeh Askari¹ · Amirreza Fateh¹ · Mohammad Reza Mohammadi^{1, *}

the date of receipt and acceptance should be inserted later

Abstract

In the context of few-shot classification, the goal is to train a classifier using a limited number of samples while maintaining satisfactory performance. However, traditional metric-based methods exhibit certain limitations in achieving this objective. These methods typically rely on a single distance value between the query feature and support feature, thereby overlooking the contribution of shallow features. To overcome this challenge, we propose a novel approach in this paper. Our approach involves utilizing multi-output embedding network that maps samples into distinct feature spaces. The proposed method extract feature vectors at different stages, enabling the model to capture both global and abstract features. By utilizing these diverse feature spaces, our model enhances its performance. Moreover, employing a self-attention mechanism improves the refinement of features at each stage, leading to even more robust representations and improved overall performance. Furthermore, assigning learnable weights to each stage significantly improved performance and results. We conducted comprehensive evaluations on the MiniImageNet and FC100 datasets, specifically in the 5-way 1-shot and 5-way 5-shot scenarios. Additionally, we performed a cross-domain task from MiniImageNet to the CUB dataset, achieving high accuracy in the testing domain. These evaluations demonstrate the efficacy of our proposed method in comparison to state-of-the-art approaches.

<https://github.com/FatemehAskari/MSENet>

Keywords Few-shot classification · Self-attention · Feature Extraction · Embedding network · Metric-based methods

1 Introduction

In recent years, deep learning has led to remarkable progress in the image recognition field, surpassing traditional computer vision algorithms [1, 2]. However, the success of deep learning models heavily relies on huge amount of data. When the available data is insufficient, the model faces difficulties in effectively optimizing its parameters [3], which can lead to overfitting. Consequently, achieving effective recognition becomes challenging, hindering the desired outcome [4, 5]. Depending on the contexts, the process of labeling images can be time-consuming and costly [6, 7]. For this reason, having models that can achieve acceptable performance with a small number of samples is perceived to be of great importance [8].

Data augmentation is one of the techniques used in situation where the amount of labeled data is insufficient [9]. However, its impact on the model's performance is limited because methods such as rotation, noise addition and scaling cannot provide new information and only help to some extent in preventing overfitting [10]. Another technique is transfer learning [11], which transfer knowledge from a source domain to a target by freezing the shallow network and fine-tuning the deep network layers. However, if the target domain differs significantly from the source domain, this approach may not be very effective when dealing with a small number of samples [12].

To address the limitation of traditional deep learning models, which performed well with large training

¹School of Computer Engineering, Iran University of Science and Technology (IUST), Tehran, Iran

E-mail: mrmohammadi@iust.ac.ir

*Corresponding author

datasets, models were developed to perform well with a fewer number of samples. One of the most important approaches is meta-learning [13]. Meta-learning aims to create models that can generalize across different tasks and rapidly adapt to new problem domain by leveraging prior learning experiences [14, 15]. The three main meta-learning approaches are: model-based meta-learning, optimization-based meta-learning, and metric-based meta-learning [16]. Model-based methods, aiming for rapid learning, primarily concentrate on model architectures and adjust model parameters based on the given tasks. Commonly used architectures in model-based methods include convolutional neural networks (CNNs) and recurrent neural networks (RNNs) [17]. Optimization-based methods aim to improve model initialization and gradient descent direction through episodic training, enabling effective learning with a small number of training samples. These methods consist of a task-specific learner and a meta-learner, trained on task distributions, to optimize model parameters for few-shot learning tasks [18, 19]. Metric-based methods focus on learning a distance metric that effectively measures the similarity between samples, with the goal of optimizing it for new learning tasks. In the context of few-shot image classification, these methods aim to ensure that samples from the same class have a small distance, while samples from different classes have a large distance [20, 21].

Metric-based methods extract feature vectors and measure the distance between classes based on these extracted vectors. However, metric-based methods usually learn only one embedding space. Gao et al. [22] proposed a multi-distance metric network that embeds samples into different spaces by extracting feature vectors at different stages. The shallow network layers capture global information about the images, while the deeper layers focus more on abstract features. Utilizing these different spaces has improved the performance of the model. In addition on different embedding spaces, it is also important to have feature vectors that are rich information. Afrasiyabi et al. [23] proposed a set-feature extractor (SetFeat) that utilizes a self-attention mechanism to obtain a richer feature space.

In this study, the proposed model integrates various components to achieve enhanced performance: The proposed method utilizes ResNet18 as the feature extractor, extracting feature maps from five different stages of ResNet18 to facilitate multi-scale representation. At each stage, we introduce learnable parameter weights to augment the model’s capacity for feature representation. Moreover, to enrich the feature space and further enhance multi-scale representation, self-attention mechanisms are incorporated into each feature map.

Though a comprehensive evaluation, we demonstrate the effectiveness of our model under MiniImageNet, CUB, and FC100 datasets.

Our contribution can be summarized as follow:

- We extracted five feature maps from backbone in order to capture both global and task specific features.
- We employ a self-attention mechanism for each feature map obtained from every stage in order to capture more valuable information.
- We incorporate learnable weights at each stage.
- We propose a novel few-shot classification. We have significantly improved the accuracy on the MiniImageNet and FC100 datasets.

2 Related Works

In this section, we discuss related work on some approaches in meta-learning.

Model-based:

Cai et al. [24] proposed Memory Matching Networks (MM-Net) for one-shot image recognition, which is based on the principles of Matching Networks [25]. MM-Net combines Convolutional Neural Networks with memory modules to leverage knowledge from a set of labeled images. It employs a contextual learner to predict CNN parameters for unlabeled images. Munkhdalai et al. [26] proposed model, called MetaNet, consists of two main components: a base learner operating in the task space and a meta learner operating in the meta space. By leveraging meta information, MetaNet can dynamically adjust its weights to recognize new concepts in the input task. Garnelo et al. [27] introduces a model called Conditional Neural Processes (CNPs), which combines deep neural networks with Bayesian methods. CNPs are capable of making accurate predictions after observing only a few training data points, while also being able to handle complex functions and large datasets. The disadvantage of model-based approaches is that they are computationally expensive and require significant computational resources.

Optimization-based:

Finn et al. [28] proposed a model-agnostic meta-learning (MAML) algorithm for fast adaptation of deep networks. The algorithm involves meta-training the model on various tasks using gradient descent to optimize its initial parameters. In the meta-testing phase, the model’s performance is evaluated on new tasks sampled from a task distribution. Through gradient-based adaptation, the model fine-tunes its parameters using a small amount of data from each new task. Sun et al. [29] proposed a novel method called Meta-Transfer Learning (MTL). MTL

combines transfer learning and meta-learning to improve the convergence and generalization of deep neural networks in low-data scenarios. It introduces scaling and shifting operations to transfer knowledge across tasks. Experimental results demonstrate the effectiveness of MTL in various few-shot learning benchmarks. The disadvantage of optimization-based approaches is that they are susceptible to issues such as getting stuck in saturation points and sensitivity to zero-gradient problems. These issues can hinder the optimization process and affect the overall performance of the method.

Metric-based:

Koch et al. [30] proposed a Siamese network that utilizes the VGG network as an extractor. They feed two pairs of images into the shared-weight convolutional network, and the network outputs a numerical value between 0 and 1, representing the similarity between the two images. Vinyals et al. [25] proposed a matching network that computes the probability distribution over labels using an attention kernel. The attention kernel calculates the cosine similarity between the support set of embedded vectors and the query. It then normalizes the similarity using the softmax formula. Snell et al. [31] proposed the Prototypical network, where each class in the support set is represented by a prototype, defined as the mean of the embedded vectors belonging to that class. The similarity between the query image’s embedded vector and the prototypes of each class is determined using the Euclidean distance. This enables the classification of query images into their respective classes. Sung et al. [32] proposed the Relation Network, which does not rely on a separate distance function. Instead, it connects the representations of the support set and the query directly within the neural network architecture, allowing the network to learn the similarity measure. Previous few-shot image classification methods commonly used four-layer convolutional networks as backbones. However utilization of pre-trained networks such as ResNet12 and ResNet18 has become much more popular nowadays. However, calculating similarities and differences to a single feature vector is not sufficient. Gao et al. [22] proposed a model called MDM-Net for few-shot learning. The MDM-Net maps input samples into four different feature spaces using a multi-output embedding network. Additionally, they introduced a task-adaptive margin to adjust the distance between different sample pairs. While previous approaches commonly used CNNs as feature extractors, there is a growing trend towards utilizing Transformers and attention mechanisms. CNNs have limitations such as a limited receptive field and parameter inefficiency. On the other hand, Transformers

offer advantages including the ability to capture long-range dependencies, model non-local relationships, and parallelize computations efficiently. They also provide interpretability by highlighting important regions or features in the input data, aiding in the understanding of the model’s decision-making process. The MDM-Net introduces a promising approach in few-shot learning by leveraging the strengths of Transformers and attention mechanisms while addressing the limitations of CNNs.

Wang et al. [33] propose a unified Query-Support Transformer (QSFormer) model for few-shot learning. The QSFormer model addresses the challenges of consistent image representations in both support and query sets, as well as effective metric learning between these sets. It consists of a sampleFormer branch that captures sample relationships and conducts metric learning using Transformer encoders, decoders, and cross-attention mechanisms. Additionally, a local patch Transformer (patchFormer) module is incorporated to extract structural representations from local image patches. The proposed model also introduces a Cross-scale Interactive Feature Extractor (CIFE) as an effective backbone module for extracting and fusing multi-scale CNN features. The QSFormer model demonstrates superior performance compared to existing methods in few-shot learning. Ran et al. [33] propose a novel deep transformer and few-shot learning (DT-FSL) framework for hyperspectral image classification. The framework aims to achieve fine-grained classification using only a few-shot instances. By incorporating spatial attention and spectral query modules, the framework captures the relationships between non-local spatial samples and reduces class uncertainty. The network is trained using episodes and task-based learning strategies to enhance its modeling capability. Additionally, domain adaptation techniques are employed to reduce inter-domain distribution variation and achieve distribution alignment.

3 Proposed method

3.1 Problem definition

The goal of few-shot classification is to classify a unseen sample. We have two datasets, D_{train} and D_{test} , each associated with corresponding class sets C_{train} and C_{test} , respectively. It is important the class sets C_{train} and C_{test} are disjoint, meaning they have no elements in common. Formally, we can express this as $C_{train} \cap C_{test} = \emptyset$. Each training episode consists of a support set S and a query set Q . The support set S comprises K examples for each of N distinct classes, denoted as $X_i^S = \{(x_{ij}^s, C = i)\}_{i=1}^K$, where x_{ij}^s represents the j th example belonging to class i . The query set Q

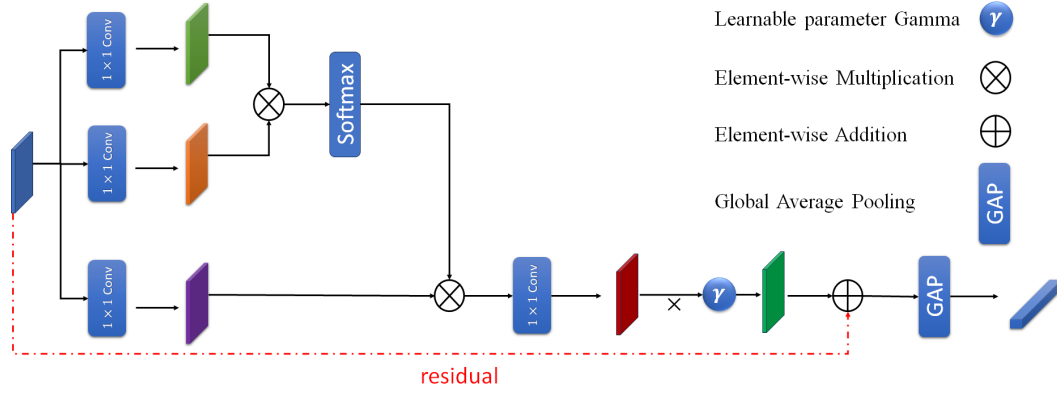


Fig. 1: SA module

contains $X^q = \{x_i^q\}_{i=1}^{n_q}$. The objective of the model is to leverage the support set S to correctly classify the query example x_i^q . In other words, the model is trained to predict the class label of the query image based on the set of supporting examples and their class affiliations provided in S . During training, each episode consists of a random sample drawn from the training dataset D_{train} . The objective of the model is to learn to extract feature representations from the examples in the support set S , such that the distance between the feature vector of the query image x_i^q and the feature vectors of the support examples $x_{i_j}^s$ can be effectively measured. Specifically, the model learns to extract discriminative feature vectors from the support examples, which can then be used to classify the query image based on its proximity to the support set features. This training paradigm encourages the model to rapidly adapt its feature extraction and classification capabilities from the limited support data to accurately predict the class label of the query instance. Similarly, during evaluation, the performance of the trained model is assessed on the held-out test dataset D_{test} . In this phase, the model extracts feature vectors for each example in the test set, leveraging the knowledge and feature extraction capabilities it learned during the training episodes on the D_{train} dataset.

3.2 Overview

The overall architecture of our model is illustrated in fig. 2. Our proposed approach incorporates several key components designed to enhance performance. At the core is a robust backbone architecture that enables the extraction of feature maps across diverse spatial scales. Additionally, we have integrated an attention module to further refine the feature extraction process. Underpinning our framework is a distance metric that facilitates effective similarity computation between inputs. More-

over, we have incorporated learnable weights to capture the relative significance of each extracted feature map.

3.2.1 Backbone

We utilized a pre-trained ResNet-18 network with initial weights from the ImageNet dataset. We removed the last fully-connected layer and fine-tuned the network on our specific dataset. To leverage multi-level feature maps, we proposed a multi-output embedding approach where we extracted feature maps at the end of each of the 5 convolutional blocks in the ResNet-18 architecture. This allowed us to capture feature representations at multiple scales and resolutions. Each sample in the support set, denoted as $x_{i_j}^s$, is mapped to five different feature spaces like $f_{i_j}^s$ as shown in equation 1:

$$f_{i_j}^s = \{f_{i_j}^{Conv1-s}, f_{i_j}^{Conv2-s}, \dots, f_{i_j}^{Conv5-s}\} \quad (1)$$

Similarly, each query sample, denoted as x_i^q , is mapped to the following feature space (equation 2):

$$f_i^q = \{f_i^{Conv1-q}, f_i^{Conv2-q}, \dots, f_i^{Conv5-q}\} \quad (2)$$

In our proposed approach, we employ multiple convolutional layers ($Conv1, Conv2, Conv3, Conv4, Conv5$) from the ResNet-18 network to extract features from the samples. Each of these convolutional blocks contributes to a distinct feature representation, allowing us to leverage different levels of abstraction and information contained in the feature maps for both the support and query samples. This multi-level feature extraction strategy enables a more comprehensive and robust representation of the input images, which is crucial for effective similarity computation and classification tasks.

3.2.2 Attention module

After extracting the feature vectors at each stage, we utilize self-attention and global average pooling. The

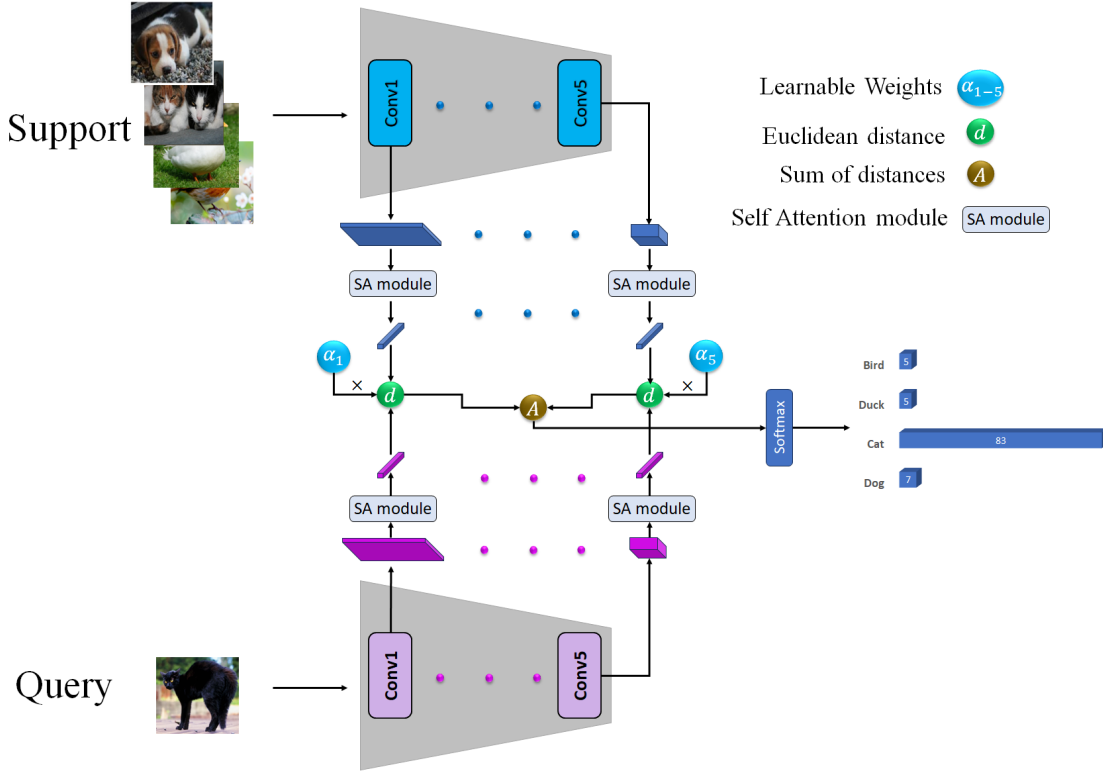


Fig. 2: Final model

representation of the attention module is illustrated in fig. 1. Considering the extracted feature vectors, we apply a 1×1 convolution on f , resulting in convolutional vectors k, g and h . This operation is performed to reduce the number of channels (equation 3):

$$k', v', q' = \text{Conv}_{1 \times 1}(f^{\text{Conv-p}}), p \in [1 - 5] \quad (3)$$

After obtaining the convolutional vectors $q'(f^{\text{Conv-p}})$ and $k'(f^{\text{Conv-p}})$, we apply the softmax function (equation 4):

$$\beta_{i,j} = \frac{\exp(S_{i,j})}{\sum_{i=1}^N \exp(S_{i,j})}, \quad \text{where } S_{i,j} = \quad (4)$$

$$q'(f_i^{\text{Conv-p}})^T k'(f_j^{\text{Conv-p}})$$

The attention mechanism computes weights β , that determine the relative importance of each pixel in the feature map. These weights are calculated across the entire spatial extent, allowing the attention module to capture long-range dependencies beyond a local neighborhood, unlike traditional convolutions. The output of the self-attention layer is computed as equation 5:

$$o^{\text{Conv-p}} = \text{Conv}_{1 \times 1} \left(\sum_{i=1}^N \beta_{i,j} v'(f_j^{\text{Conv-p}}) \right) \quad (5)$$

In equation 5, in addition to using various ResNet18 blocks for feature extraction, we employ a 1×1 convolution layer twice - once before applying the attention mechanism and again after it. The purpose of using the 1×1 convolution layer twice is to make the network more nonlinear and to allow us to leverage the previous information more evenly. The scaling factor, typically denoted as γ , is a learnable parameter in the network that is multiplied with the input feature map $f^{\text{Conv-p}}$ before the addition (equation 6):

$$y^{\text{Conv-p}} = \gamma \times o_i + f^{\text{Conv-p}} \quad (6)$$

After obtaining the final output, we take a global average pooling. The output is represented for each query and support sample as follows:

$$f'_{ij}{}^s = \{f'_{ij}{}^{\text{Conv1-s}}, f'_{ij}{}^{\text{Conv2-s}}, \dots, f'_{ij}{}^{\text{Conv5-s}}\} \quad (7)$$

$$f'_{ij}{}^q = \{f'_i{}^{\text{Conv1-q}}, f'_i{}^{\text{Conv2-q}}, \dots, f'_i{}^{\text{Conv5-q}}\} \quad (8)$$

3.2.3 Distance metric

Once we have obtained the final output from the previous stage, we take the average of the vectors from all the support samples belonging to the same class to obtain

the prototypes for each class from the support set as equations 9 .

$$c_i^{Conv-p} = \frac{1}{|K|} \sum_{j=1}^K f_{ij}^{Conv-p-s}, \text{ where } p \in [1-5] \quad (9)$$

We calculate the Euclidean distance between the feature map of each query sample f_i^{Conv-p} and its corresponding prototype map c_j^{Conv-p} , considering 5 feature maps per sample, as described in equation 10.

$$d_{i,j}^{Conv-p} = \text{Euclidean} \left(f_i^{Conv-p}, c_j^{Conv-p} \right) \quad (10)$$

3.2.4 Learnable weights

Considering the emphasis of shallow network layers on global features and deep layers on abstract features, we opted to assign weights to the distances computed in the five feature spaces for each query sample-support set representative pair. These weights are trainable within the network, and their initial assignment significantly influences the model’s performance, which will be elaborated on in the Experiment section. The final distance is obtained by aggregating the weighted distances from these five feature spaces as shown in Equation 11:

$$d_{i,j} = \sum_{r=1}^5 w_{i,j}^{Conv-p} \times d_{i,j}^{Conv-p}, \quad p \in [1-5] \quad (11)$$

Afterward, we apply softmax as shown in Equation 12:

$$p(y = j | x_i^q) = \frac{\exp(-d_{i,j})}{\sum_{l=1}^{n_s} \exp(-d_{i,l})} \quad (12)$$

The learning process involves minimizing the negative log-probability $J = -\log p(y = j | x_i^q)$ of the true class j using the Adam optimizer. Training episodes are formed by randomly selecting a subset of classes from the training set. Within each selected class, a subset of examples is chosen to form the support set, while another subset from the remaining examples is used as query points.

4 Experimental Results

4.1 Datasets

The proposed method was evaluated on three widely used datasets commonly employed for few-shot learning tasks: MiniImageNet [65], FC100 [66], and CUB [67].

MiniImageNet dataset. The MiniImageNet is a subset of the ImageNet dataset designed for training and evaluating machine learning models. This dataset contains 100 classes with 600 images per class. The images are randomly divided into three splits: 64 classes

for training, 16 classes for validation, and 20 classes for testing. This data partitioning allows researchers to evaluate how effectively models can generalize to new and unseen classes after being trained on the provided set of classes.

FC100 dataset. The FC100 is another dataset similar in structure to MiniImageNet. It contains 100 classes with 600 images per class. However, the class splits are handled differently - the 100 classes are randomly divided into 60 training classes, 20 validation classes, and 20 test classes. This ensures that the training, validation, and test sets are entirely disjoint, which can provide a more realistic evaluation of a model’s ability to learn general visual representations.

CUB dataset. The CUB (Caltech-UCSD Birds-200-2011) dataset is a collection of bird images often used for fine-grained visual classification tasks. This dataset contains 200 different bird species, with a total of 11,788 images. The images are randomly partitioned into 100 training classes, 50 validation classes, and 50 test classes. This dataset poses a challenging problem as many bird species can appear visually similar, requiring models to learn discriminative features to accurately classify the different species.

4.2 Experimental setting

For our datasets, we performed the following preprocessing and model configuration steps. First, all input images were resized to a resolution of 84 x 84 pixels. Regarding the model architecture, we employed a pre-trained ResNet-18 as the backbone feature extractor. Specifically, we extracted features from the 5 stages of the ResNet-18 network, obtaining feature maps from each of these stages.

For the optimization of our models, we employed the Adam optimizer. For the MiniImageNet dataset, we used a constant learning rate of 10^{-4} , while for the FC100 dataset, the learning rate was 2×10^{-5} . This learning rate was selected based on preliminary experiments to ensure stable and efficient convergence of the models during training. All experiments were conducted on an NVIDIA RTX 4090 GPU system.

4.3 Evaluation metric

To evaluate the performance of our models, we employed the following scenario: For the training phase, we sampled 30 random classes and 5 examples per class from the training set. We then trained the model on these samples. For evaluation, we tested the trained model on a 5-way 5-shot task by selecting 5 random classes and

Table 1: Evaluation on MiniImageNet in 5-way.

Method	Backbone	1-shot	5-shot
AdaResNet [34]	ResNet12	56.88	71.94
TADAM [35]	ResNet12	58.50	76.70
MetaOptNet [36]	ResNet12	62.64	78.63
Neg-Margin [37]	ResNet12	63.85	81.57
MixtFSL [38]	ResNet12	63.98	82.04
Meta-Baseline [39]	ResNet12	63.17	79.26
FRN [40]	ResNet12	66.45	82.83
QSFormer [41]	ResNet12	65.24	79.96
Distill [42]	ResNet12	64.82	82.14
Meta-Baseline + DiffKendall [43]	ResNet12	65.56	80.79
LEO [44]	WRN-28-10	61.76	77.59
CC+rot [45]	WRN-28-10	62.93	79.87
FEAT [46]	WRN-28-10	65.10	81.11
Neg-Cosine [47]	ResNet18	62.33	80.94
MixtFSL [48]	ResNet18	60.11	77.76
MergeNet-Concat [49]	ResNet18	65.05	77.76
Our model	ResNet18	66.57	84.42

Table 2: Evaluation on FC100 in 5-way.

Method	Backbone	1-shot	5-shot
P-Net [31]	ResNet12	37.80	53.30
Cosine Classifier [50]	ResNet12	38.47	57.67
TADAM [51]	ResNet12	40.10	56.10
SimpleShot [52]	ResNet10	40.13	53.63
Metaopt Net [53]	ResNet12	41.10	55.50
DC [54]	ResNet12	42.04	57.63
MDM-Net [55]	ResNet12	43.62	57.41
RFS [56]	ResNet12	44.60	60.90
SSFormers [57]	ResNet12	43.72	58.92
LSFSL [58]	ResNet12	43.60	60.12
Barlow Twins + DSA [59]	ViT-B	41.42	55.47
Our model	ResNet18	44.78	66.27

using 5 examples per class. This process was repeated over multiple episodes to compute the overall 5-way 5-shot accuracy. Additionally, we evaluated the models on a 5-way 1-shot task. In this setting, we followed a similar approach but used only 1 example per class during the evaluation phase. Our primary evaluation metric for both tasks was accuracy.

4.4 Comparison with state of the arts

Based on the results presented in Table 1 and Table 2, our proposed model demonstrates strong few-shot learning performance compared to the state-of-the-art

Table 3: The comparison of our model’s performance against state-of-the-art methods on the test domain CUB.

Method	1-shot	5-shot
RelatonNet [60]	35.21	51.10
MatchingNet [61]	42.28	57.21
RelationNet+LFT [62]	48.10	65.02
MatchingNet+LFT [62]	43.38	61.44
RelationNet+ATA [63]	48.49	59.42
StyleAdv [64]	48.49	68.72
StyleAdv-FIT [64]	-	70.90
Our model	52.95	71.59

approaches. As shown in Table 1, on the MiniImageNet dataset, our model achieves an accuracy of 66.57 in the 1-shot setting and 84.42 in the 5-shot setting. This indicates that our model is able to effectively leverage the limited training data and rapidly adapt to new tasks, showcasing its superior few-shot learning capabilities. Similarly, on the more challenging FC100 dataset, as shown in Table 2, our model outperforms the existing state-of-the-art methods by a significant margin, obtaining an accuracy of 44.78 in the 1-shot setting and 66.27 in the 5-shot setting. The consistent improvements observed across both MiniImageNet and FC100 datasets highlight the effectiveness of the design choices and techniques employed in our model. These choices and techniques allow it to learn more robust and transferable representations for few-shot learning

Table 4: The influence of each component to the model’s performance

baseline	Multiscale	Learnable Weight	Self-attention	MiniImageNet		FC100	
				1 shot	5 shot	1 shot	5 shot
✓	X	X	X	62.83	82.38	39.47	63.44
✓	✓	X	X	63.65	83.23	41.97	64.8
✓	✓	✓	X	64.73	83.92	43.7	65.76
✓	✓	✓	✓	66.57	84.42	44.78	66.27

Table 5: The influence of different weights at each stage on the model’s performance on MiniImageNet

	Weights					1 shot		5 shot	
	w1	w2	w3	w4	w5	accuracy without learnable weights	accuracy with learnable weights	accuracy without learnable weights	accuracy with learnable weights
Weight Initialization	1	1	1	1	1	63.80%	64.54%	82.24%	82.99%
	1	1.1	1.2	1.3	1.4	63.34%	64.73%	83.02%	83.92%
	1	1.2	1.4	1.6	1.8	62.13%	64.6%	83.68%	83.70%

scenarios. These results position our model as a highly competitive approach in the field of few-shot learning.

4.5 Cross domain

To further assess the generalization capabilities of our model, we conducted a cross-domain evaluation using the CUB dataset as the testing domain, while the MiniImageNet dataset was used for training. As shown in Table 3, our model demonstrated strong performance in this challenging cross-domain few-shot learning setting. Specifically, our model achieved an impressive 1-shot accuracy of 52.95 and a 5-shot accuracy of 71.59 on the CUB dataset. This outperforms various state-of-the-art approaches, such as RelationNet+LFT, MatchingNet+LFT, and the strong Baseline model, showcasing the superior ability of our approach to adapt to the distributional shift between the training and testing domains. The consistent improvement over the competing methods across both the 1-shot and 5-shot settings highlights the robustness and transferability of the representations learned by our model. This demonstrates its effectiveness in tackling the challenging cross-domain few-shot learning problem, where the model must generalize its knowledge from the training domain to the novel testing domain. These results further solidify the position of our model as a highly competitive and versatile few-shot learning solution.

4.6 Ablation study

To better understand the contributions of different components in our model, we conducted an ablation study and reported the results. Table 4 illustrates the influence of individual components on overall model performance. The Baseline configuration, serving as the foundation of our model, achieves notable results with 62.83% accuracy for the 1-shot task and 82.38% for the 5-shot task on the MiniImageNet dataset. On the FC100 dataset, the Baseline configuration results in 39.47% 1-shot and 63.44% 5-shot accuracy.

Introducing the Multiscale module, which enhances feature extraction by capturing information at multiple scales, leads to improvements in both 1-shot and 5-shot performance across both datasets. Adding the Learnable Weight component, which adapts weights for different feature channels, further boosts accuracy, demonstrating its effectiveness.

The final inclusion of the Self-attention module results in the best overall performance, with the model achieving 66.57% accuracy for the 1-shot task and 84.42% for the 5-shot task on MiniImageNet. On FC100, the performance reaches 44.78% for 1-shot and 66.27% for 5-shot tasks. These results underscore the significant contribution of the self-attention mechanism to enhancing the few-shot learning capabilities of our approach.

As shown in Table 5, two important observations can be made regarding model performance on the MiniImageNet dataset:

1) Advantage of Learnable Weights: The results indicate a clear benefit to using learnable weights. In both

the 5-way 1-shot and 5-way 5-shot tasks, models with learnable weights achieved higher accuracies compared to those with fixed weights. For example, in the 5-way 1-shot task, accuracy increased from 63.80% to 64.54% when weights were learnable. Similarly, in the 5-way 5-shot task, accuracy improved from 82.24% to 82.99% with learnable weights. These results demonstrate that incorporating learnable weights significantly enhances model performance.

2) Impact of Weight Initialization: The choice of weight initialization also plays a crucial role in model performance. The best results were observed with initial weights set to 1.1, 1.2, 1.3, and 1.4. This variation underscores the importance of proper weight initialization in achieving optimal model accuracy.

In summary, Table 5, highlights that both the use of learnable weights and careful selection of weight initialization are key factors in improving model performance.

Table 6: The influence of different gamma at each stage on the model’s performance on MiniImageNet

Gamma 1	Gamma 2	1 shot	5 shot
0.2	0.2	66.57%	84.42%
0.3	0.3	65.09%	84.12%
0.4	0.4	65.15%	84.16%

As shown in Table 6, the impact of different γ values on model performance in the self-attention module is evident for both 1-shot and 5-shot tasks. Specifically, setting γ values to 0.2 for both support and query images resulted in the highest accuracy. This indicates that the choice of γ significantly influences model performance, with the 0.2 setting yielding the best results compared to other tested values.

5 Conclusion

This paper presents an innovative strategy to enhance few-shot classification by integrating a self-attention network and embedding learnable weights at each stage, leading to improved performance and substantial outcomes. Through feature vector extraction and weight transfer across stages, this technique elevates multi-scale feature representation, thereby enhancing overall performance. Moreover, the incorporation of self-attention mechanisms refines features at each stage, resulting in more robust representations and enhanced performance. The introduction of learnable weights at each stage significantly boosts performance and outcomes. Extensive

evaluations on the MiniImageNet and FC100 datasets underscore the efficacy of this method compared to current state-of-the-art approaches.

References

1. A. Saber, P. Parhami, A. Siahkarzadeh, and A. Fateh, “Efficient and accurate pneumonia detection using a novel multi-scale transformer approach,” *arXiv preprint arXiv:2408.04290*, 2024.
2. A. Fateh, R. T. Birgani, M. Fateh, and V. Abolghasemi, “Advancing multilingual handwritten numeral recognition with attention-driven transfer learning,” *IEEE Access*, vol. 12, pp. 41 381–41 395, 2024.
3. A. Sharif Razavian, H. Azizpour, J. Sullivan, and S. Carlsson, “Cnn features off-the-shelf: An astounding baseline for recognition,” pp. 806–813, 2014.
4. S. Rezvani, F. S. Siahkar, Y. Rezvani, A. A. Gharahbagh, and V. Abolghasemi, “Single image denoising via a new lightweight learning-based model,” *IEEE Access*, 2024.
5. X. Zhang, J. Zhou, W. Sun, and S. K. Jha, “A lightweight cnn based on transfer learning for covid-19 diagnosis,” *Computers, Materials & Continua*, vol. 72, no. 1, 2022.
6. A. Fateh, M. Fateh, and V. Abolghasemi, “Enhancing optical character recognition: Efficient techniques for document layout analysis and text line detection,” *Engineering Reports*, vol. 6, no. 9, p. e12832, 2024.
7. A. Fateh, M. Rezvani, A. Tajary, and M. Fateh, “Persian printed text line detection based on font size,” *Multimedia Tools and Applications*, vol. 82, no. 2, pp. 2393–2418, 2023.
8. Y. Wang, Q. Yao, J. T. Kwok, and L. M. Ni, “Generalizing from a few examples: A survey on few-shot learning,” *ACM computing surveys (csur)*, vol. 53, no. 3, pp. 1–34, 2020.
9. S. Yang, W. Xiao, M. Zhang, S. Guo, J. Zhao, and F. Shen, “Image data augmentation for deep learning: A survey,” *arXiv preprint arXiv:2204.08610*, 2022.
10. J. Zhou, Y. Zheng, J. Tang, J. Li, and Z. Yang, “Flipda: Effective and robust data augmentation for few-shot learning,” *arXiv preprint arXiv:2108.06332*, 2021.
11. D. Xue, X. Zhou, C. Li, Y. Yao, M. M. Rahaman, J. Zhang, H. Chen, J. Zhang, S. Qi, and H. Sun, “An application of transfer learning and ensemble learning techniques for cervical histopathology image classification,” *IEEE Access*, vol. 8, pp. 104 603–104 618, 2020.
12. H. Xia, H. Zhao, and Z. Ding, “Adaptive adversarial network for source-free domain adaptation,” pp. 9010–9019, 2021.
13. Y. Wang, Q. Yao, J. T. Kwok, and L. M. Ni, “Generalizing from a few examples: A survey on few-shot learning,” *ACM computing surveys (csur)*, vol. 53, no. 3, pp. 1–34, 2020.
14. K. He, N. Pu, M. Lao, and M. S. Lew, “Few-shot and meta-learning methods for image understanding: a survey,” *International Journal of Multimedia Information Retrieval*, vol. 12, no. 2, p. 14, 2023.
15. M. Goldblum, L. Fowl, and T. Goldstein, “Adversarially robust few-shot learning: A meta-learning approach,” *Advances in Neural Information Processing Systems*, vol. 33, pp. 17 886–17 895, 2020.
16. A. Parnami and M. Lee, “Learning from few examples: A summary of approaches to few-shot learning,” *arXiv preprint arXiv:2203.04291*, 2022.

17. L. Sun, W. Li, X. Ning, L. Zhang, X. Dong, and W. He, "Gradient-enhanced softmax for face recognition," *IEICE TRANSACTIONS on Information and Systems*, vol. 103, no. 5, pp. 1185–1189, 2020.
18. W. Bian, Y. Chen, X. Ye, and Q. Zhang, "An optimization-based meta-learning model for mri reconstruction with diverse dataset," *Journal of Imaging*, vol. 7, no. 11, p. 231, 2021.
19. H. Cho, Y. Cho, J. Yu, and J. Kim, "Camera distortion-aware 3d human pose estimation in video with optimization-based meta-learning," pp. 11 169–11 178, 2021.
20. M. J. Lee and J. So, "Metric-based learning for nearest-neighbor few-shot image classification," pp. 460–464, 2021.
21. P. Li, G. Zhao, and X. Xu, "Coarse-to-fine few-shot classification with deep metric learning," *Information Sciences*, vol. 610, pp. 592–604, 2022.
22. F. Gao, L. Cai, Z. Yang, S. Song, and C. Wu, "Multi-distance metric network for few-shot learning," *International Journal of Machine Learning and Cybernetics*, vol. 13, no. 9, pp. 2495–2506, 2022.
23. A. Afrasiyabi, H. Larochelle, J.-F. Lalonde, and C. Gagné, "Matching feature sets for few-shot image classification," pp. 9014–9024, 2022.
24. Q. Cai, Y. Pan, T. Yao, C. Yan, and T. Mei, "Memory matching networks for one-shot image recognition," pp. 4080–4088, 2018.
25. O. Vinyals, C. Blundell, T. Lillicrap, D. Wierstra *et al.*, "Matching networks for one shot learning," *Advances in neural information processing systems*, vol. 29, 2016.
26. T. Munkhdalai and H. Yu, "Meta networks," pp. 2554–2563, 2017.
27. M. Garnelo, D. Rosenbaum, C. Maddison, T. Ramalho, D. Saxton, M. Shanahan, Y. W. Teh, D. Rezende, and S. A. Eslami, "Conditional neural processes," pp. 1704–1713, 2018.
28. C. Finn, P. Abbeel, and S. Levine, "Model-agnostic meta-learning for fast adaptation of deep networks," pp. 1126–1135, 2017.
29. Q. Sun, Y. Liu, T.-S. Chua, and B. Schiele, "Meta-transfer learning for few-shot learning," pp. 403–412, 2019.
30. G. Koch, R. Zemel, R. Salakhutdinov *et al.*, "Siamese neural networks for one-shot image recognition," vol. 2, no. 1, 2015.
31. J. Snell, K. Swersky, and R. Zemel, "Prototypical networks for few-shot learning," *Advances in neural information processing systems*, vol. 30, 2017.
32. F. Sung, Y. Yang, L. Zhang, T. Xiang, P. H. Torr, and T. M. Hospedales, "Learning to compare: Relation network for few-shot learning," pp. 1199–1208, 2018.
33. X. Wang, X. Wang, B. Jiang, and B. Luo, "Few-shot learning meets transformer: Unified query-support transformers for few-shot classification," *IEEE Transactions on Circuits and Systems for Video Technology*, 2023.
34. T. Munkhdalai, X. Yuan, S. Mehri, and A. Trischler, "Rapid adaptation with conditionally shifted neurons," in *International conference on machine learning*. PMLR, 2018, pp. 3664–3673.
35. B. Oreshkin, P. Rodríguez López, and A. Lacoste, "Tadam: Task dependent adaptive metric for improved few-shot learning," *Advances in neural information processing systems*, vol. 31, 2018.
36. K. Lee, S. Maji, A. Ravichandran, and S. Soatto, "Meta-learning with differentiable convex optimization," in *Proceedings of the IEEE/CVF conference on computer vision and pattern recognition*, 2019, pp. 10 657–10 665.
37. B. Liu, Y. Cao, Y. Lin, Q. Li, Z. Zhang, M. Long, and H. Hu, "Negative margin matters: Understanding margin in few-shot classification," in *Computer Vision–ECCV 2020: 16th European Conference, Glasgow, UK, August 23–28, 2020, Proceedings, Part IV 16*. Springer, 2020, pp. 438–455.
38. A. Afrasiyabi, J.-F. Lalonde, and C. Gagné, "Mixture-based feature space learning for few-shot image classification," in *Proceedings of the IEEE/CVF international conference on computer vision*, 2021, pp. 9041–9051.
39. Y. Chen, Z. Liu, H. Xu, T. Darrell, and X. Wang, "Meta-baseline: Exploring simple meta-learning for few-shot learning," in *Proceedings of the IEEE/CVF international conference on computer vision*, 2021, pp. 9062–9071.
40. D. Wertheimer, L. Tang, and B. Hariharan, "Few-shot classification with feature map reconstruction networks," in *Proceedings of the IEEE/CVF conference on computer vision and pattern recognition*, 2021, pp. 8012–8021.
41. X. Wang, X. Wang, B. Jiang, and B. Luo, "Few-shot learning meets transformer: Unified query-support transformers for few-shot classification," *IEEE Transactions on Circuits and Systems for Video Technology*, vol. 33, no. 12, pp. 7789–7802, 2023.
42. Y. Tian, Y. Wang, D. Krishnan, J. B. Tenenbaum, and P. Isola, "Rethinking few-shot image classification: a good embedding is all you need?" in *Computer Vision–ECCV 2020: 16th European Conference, Glasgow, UK, August 23–28, 2020, Proceedings, Part XIV 16*. Springer, 2020, pp. 266–282.
43. K. Zheng, H. Zhang, and W. Huang, "Diffkendall: a novel approach for few-shot learning with differentiable kendall's rank correlation," *Advances in Neural Information Processing Systems*, vol. 36, pp. 49 403–49 415, 2023.
44. A. A. Rusu, D. Rao, J. Sygnowski, O. Vinyals, R. Pascanu, S. Osindero, and R. Hadsell, "Meta-learning with latent embedding optimization," *arXiv preprint arXiv:1807.05960*, 2018.
45. S. Gidaris, A. Bursuc, N. Komodakis, P. Pérez, and M. Cord, "Boosting few-shot visual learning with self-supervision," in *Proceedings of the IEEE/CVF international conference on computer vision*, 2019, pp. 8059–8068.
46. H.-J. Ye, H. Hu, D.-C. Zhan, and F. Sha, "Few-shot learning via embedding adaptation with set-to-set functions," in *Proceedings of the IEEE/CVF conference on computer vision and pattern recognition*, 2020, pp. 8808–8817.
47. B. Liu, Y. Cao, Y. Lin, Q. Li, Z. Zhang, M. Long, and H. Hu, "Negative margin matters: Understanding margin in few-shot classification," in *Computer Vision–ECCV 2020: 16th European Conference, Glasgow, UK, August 23–28, 2020, Proceedings, Part IV 16*. Springer, 2020, pp. 438–455.
48. A. Afrasiyabi, J.-F. Lalonde, and C. Gagné, "Mixture-based feature space learning for few-shot image classification," in *Proceedings of the IEEE/CVF international conference on computer vision*, 2021, pp. 9041–9051.
49. J. Atanbori and S. Rose, "Mergednet: A simple approach for one-shot learning in siamese networks based on similarity layers," *Neurocomputing*, vol. 509, pp. 1–10, 2022.
50. W.-Y. Chen, Y.-C. Liu, Z. Kira, Y.-C. F. Wang, and J.-B. Huang, "A closer look at few-shot classification," *arXiv preprint arXiv:1904.04232*, 2019.
51. B. Oreshkin, P. Rodríguez López, and A. Lacoste, "Tadam: Task dependent adaptive metric for improved few-shot learning," *Advances in neural information processing systems*, vol. 31, 2018.

52. Y. Wang, W.-L. Chao, K. Q. Weinberger, and L. Van Der Maaten, "SimpleShot: Revisiting nearest-neighbor classification for few-shot learning," *arXiv preprint arXiv:1911.04623*, 2019.
53. K. Lee, S. Maji, A. Ravichandran, and S. Soatto, "Meta-learning with differentiable convex optimization," in *Proceedings of the IEEE/CVF conference on computer vision and pattern recognition*, 2019, pp. 10 657–10 665.
54. Y. Lifchitz, Y. Avrithis, S. Picard, and A. Bursuc, "Dense classification and implanting for few-shot learning," in *Proceedings of the IEEE/CVF conference on computer vision and pattern recognition*, 2019, pp. 9258–9267.
55. F. Gao, L. Cai, Z. Yang, S. Song, and C. Wu, "Multi-distance metric network for few-shot learning," *International Journal of Machine Learning and Cybernetics*, vol. 13, no. 9, pp. 2495–2506, 2022.
56. Y. Tian, Y. Wang, D. Krishnan, J. B. Tenenbaum, and P. Isola, "Rethinking few-shot image classification: a good embedding is all you need?" in *Computer Vision—ECCV 2020: 16th European Conference, Glasgow, UK, August 23–28, 2020, Proceedings, Part XIV 16*. Springer, 2020, pp. 266–282.
57. H. Chen, H. Li, Y. Li, and C. Chen, "Sparse spatial transformers for few-shot learning," *Science China Information Sciences*, vol. 66, no. 11, p. 210102, 2023.
58. D. Chakravarthi Padmanabhan, S. Gowda, E. Arani, and B. Zonooz, "Lsfl: Leveraging shape information in few-shot learning," *arXiv e-prints*, pp. arXiv–2304, 2023.
59. Z. Song, W. Qiang, C. Zheng, F. Sun, and H. Xiong, "On the discriminability of self-supervised representation learning," *arXiv preprint arXiv:2407.13541*, 2024.
60. F. Sung, Y. Yang, L. Zhang, T. Xiang, P. H. Torr, and T. M. Hospedales, "Learning to compare: Relation network for few-shot learning," in *Proceedings of the IEEE conference on computer vision and pattern recognition*, 2018, pp. 1199–1208.
61. O. Vinyals, C. Blundell, T. Lillicrap, D. Wierstra *et al.*, "Matching networks for one shot learning," *Advances in neural information processing systems*, vol. 29, 2016.
62. H.-Y. Tseng, H.-Y. Lee, J.-B. Huang, and M.-H. Yang, "Cross-domain few-shot classification via learned feature-wise transformation," *arXiv preprint arXiv:2001.08735*, 2020.
63. H. Wang and Z.-H. Deng, "Cross-domain few-shot classification via adversarial task augmentation," *arXiv preprint arXiv:2104.14385*, 2021.
64. Y. Fu, Y. Xie, Y. Fu, and Y.-G. Jiang, "Styleadv: Meta style adversarial training for cross-domain few-shot learning," in *Proceedings of the IEEE/CVF Conference on Computer Vision and Pattern Recognition*, 2023, pp. 24 575–24 584.
65. O. Vinyals, C. Blundell, T. Lillicrap, D. Wierstra *et al.*, "Matching networks for one shot learning," *Advances in neural information processing systems*, vol. 29, 2016.
66. B. Oreshkin, P. Rodríguez López, and A. Lacoste, "Tadam: Task dependent adaptive metric for improved few-shot learning," *Advances in neural information processing systems*, vol. 31, 2018.
67. C. Wah, S. Branson, P. Welinder, P. Perona, and S. Belongie, "The caltech-ucsd birds-200-2011 dataset," 2011.